IOP Conf. Series: Materials Science and Engineering **1345** (2026) 012008 doi:10.1088/1757-899X/1345/1/012008

Piezometric properties of additively manufactured composites at cryogenic temperatures

T Tonge[1,2], R Howard[1,2] and S Mojumder[1,2*]

[1]School of Mechanical and Materials Engineering, [2] HYdrogen Properties for Energy Research (HYPER) Center, Washington State University, Pullman, WA 99164-2920 USA

E-mail: *satyajit.mojumder@wsu.edu

Abstract. Short carbon fiber–reinforced composites can be additively manufactured into complex geometries, providing lightweight structures with high mechanical integrity and functional properties such as piezometric response, defined as changes in resistivity and conductivity under applied loads. However, the piezometric behavior of these materials remains largely unstudied at cryogenic temperatures. This study investigates both the mechanical and piezometric properties (piezoresistivity) of additively manufactured carbon fiber-reinforced composites under cryogenic conditions. The influence of key processing parameters, including print orientation, print speed, and layer height, on these properties is analyzed and compared to performance at room temperature. The results indicate significant changes in piezometric characteristics at cryogenic temperatures based on printing parameters. These findings suggest potential applications in the structural health monitoring of cryogenic materials, utilizing the materials' responsive piezometric properties.

1. Introduction

Additive manufacturing (AM), commonly known as 3D printing, has opened new frontiers in materials development by enabling the fabrication of complex, customizable structures with precise control over geometry and internal architecture. Unlike conventional subtractive manufacturing techniques, AM offers significant advantages such as reduced material waste, shorter design-to-production cycles, and the ability to fabricate components with intricate geometries that would be difficult or impossible to produce otherwise [1]. These capabilities have driven the rapid adoption of AM technologies across a wide range of industries, including aerospace, biomedical, automotive, architecture, and consumer goods [2]. Moreover, ongoing advances in printable materials, from polymers and metals to ceramics and composites, have expanded the functionality and application scope of AM [3].

The properties of materials produced by additive manufacturing can vary significantly depending on the printing parameters. In the fused filament fabrication (FFF) process, key processing conditions such as nozzle temperature, print speed, layer height, and bed temperature play a critical role in determining the mechanical and functional behavior of the printed parts [4,5]. These parameters not only influence structural properties but also affect functional responses, including piezometric response, defined here as the change in a material's electrical resistance under applied mechanical strain (piezoresistivity) [6]. Piezometric properties are particularly important because they enable self-sensing behavior, where resistance changes provide a direct signal of stress, strain, or damage in a structure [7-10]. This functionality has potential applications in structural health monitoring, wearable sensors, and smart devices. For example, Tan et al. [11] demonstrated that in FFF-based additive manufacturing, the piezoresistive properties of printed materials varied with print speed and layer height, showing an increase in piezoresistivity at room temperature. While such studies establish that FFF processing parameters influence functional response, they primarily focus on room-temperature performance.

Expanding the range of additively manufactured materials suitable for extreme conditions is crucial for applications in aerospace, quantum computing, and space exploration [12,13]. Recent studies suggest that materials can exhibit unique behaviors at cryogenic temperatures, including changes in mechanical strength, ductility, and functional response [14]. In particular, piezometric responses may be amplified at low temperatures, where thermal contraction and reduced molecular motion intensify internal interactions. For example, decreasing the temperature has been shown to increase the resistivity of carbon black–loaded materials by several orders of magnitude [15]. However, the combined influence of processing conditions and extreme environments on the piezometric behavior of additively manufactured materials remains poorly understood.

Building on these gaps, the present study investigates how FFF printing parameters influence both the mechanical properties and piezometric responses of additively manufactured composites at room and cryogenic temperatures. Specifically, we investigate how print orientation, print speed, and layer height govern the relative change in piezometric resistance ($\Delta R/R$) when subjected to mechanical loading. By addressing this research question, we aim to establish processing–structure–property relationships that can inform the design of multifunctional materials for low-temperature sensing, structural health monitoring, and smart component integration.

2. Materials and Methods

2.1. Material and Sample Preparation

Composite specimens were manufactured using the fused filament fabrication (FFF) process, with carbon fiber reinforced polyamide 12 (PA12) from MakerBot, commercially known as Nylon 12 Carbon Fiber. The material contains a total carbon fiber volume concentration of 35%. The Prusa Pro HT90 was used to print composite tensile specimens at 100% infill density with a length of 150 mm and a thickness of 3.2 mm, following the ASTM D638 Type-IV standard [16]. Prior to printing, the filament material was dried to <15% relative humidity. The material was extruded at a temperature of 285 °C, in a heated chamber at 50 °C, and a bed plate temperature of 100 °C. The specimens were printed with a 0.4 mm hardened steel nozzle. The tensile specimens were printed varying print orientation, print speed, and layer height. The varied parameters of each specimen are provided in Table 1. A minimum of 3 tensile specimens were printed and tested for each set of parameters to ensure experimental reliability.

Table 1: Experimental design showing the parameters varied among the specimens used in this study

Parameters	**Varied Parameters**	**Fixed Parameters**
Layer Height (mm)	0.12, 0.16, 0.2	0°, 150 mm/s
Print Orientation	0°/90°, 45°/135°	0.2 mm, 150 mm/s
Print Speed (mm/s)	50, 100, 150	0.2 mm, 0°

To isolate the individual effects of each variable, we employed a controlled experimental approach where only one parameter was varied per test series while the remaining two parameters were held constant. This methodology ensures that observed differences in material properties and resistivity can be directly attributed to the specific parameter under investigation. To measure the relative changes in resistance ($\Delta R/R$), wires of the same length and gauge were soldered to the specimens using stainless steel pins outside the gauge length. A total of four electrodes were placed approximately 10 mm from each other, measuring two sets of resistance readings shown in Figure 1.

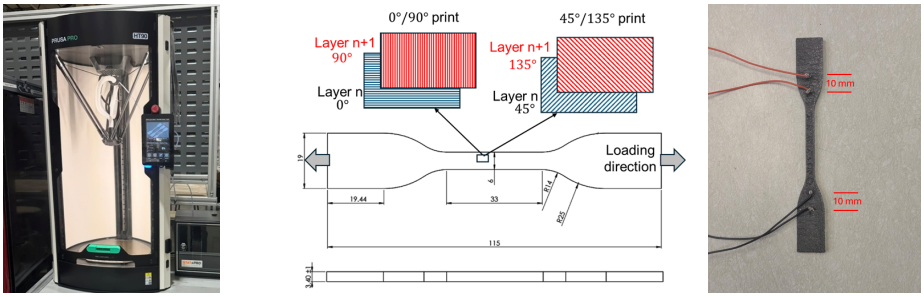

(a) (b) (c)

Figure 1: (a) Prusa Pro HT90 used for printing specimens, (b) printed specimen dimensions showing print orientations with loading direction, and (c) prepared specimen with soldered electrodes.

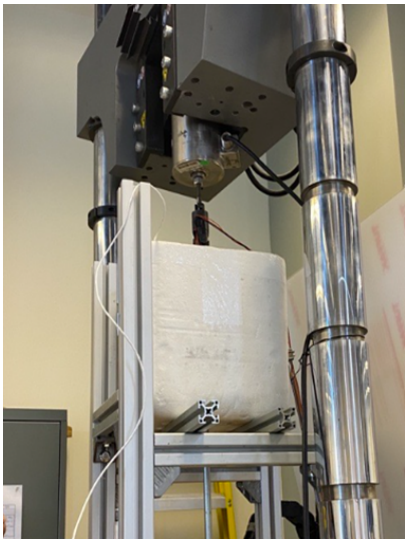

Figure 2: Loaded specimen setup for cryogenic temperature testing, showing the specimen mounted in the grips, instrumented with electrodes, and fully submerged in liquid nitrogen.

2.2. Methods

Specimens were mounted in the grips of an Instron tensile testing machine equipped with a 3000 lb load cell, ensuring secure fixation to accurately measure and record load-displacement data throughout the test. Electrical leads attached to the specimen's electrodes were connected to a digital multimeter, enabling real-time monitoring and recording of the electrical resistance changes during mechanical loading. For cryogenic temperature testing, specimens were fully submerged in liquid nitrogen (LN2) within the container illustrated in Figure 2. LN2 was continuously added until the rate of boil-off stabilized, ensuring the specimen reached a target temperature of approximately 77 K. Following thermal stabilization, axial tensile loading was applied at a controlled displacement rate of 1mm/s and 0.5mm/s for room temperature and LN2 temperature, respectively, until specimen failure. This set up allowed simultaneous acquisition of mechanical and piezometric response data under cryogenic conditions.

3. Results and Discussion

In this study, we printed samples varying print orientation, print speed, and layer height as presented in Table 1 and tested the samples for mechanical and piezometric properties both at room temperature and LN2 temperature. Although a nominal 100% infill was specified during FFF processing, some degree of porosity is unavoidable in printed components. This inherent porosity may influence the piezoresistive response by introducing local variations in stress distribution and conductive pathways, and should therefore be considered when interpreting the results. The tensile and piezometric testing results are presented and discussed in this section.

3.1. Print Orientation

Tensile tests were performed on specimens printed at $0°/90°$ and $45°/135°$ fiber orientations, and the corresponding stress-strain curves for room temperature and LN2 temperature are shown in Figure3. As expected, the $0°/90°$ specimens exhibited higher mechanical strength compared to the $45°/135°$ samples, reflecting the preferential load-bearing alignment of fibers. In room temperature, the printed samples show elasto-plastic behavior with ductile failure and necking; however, at LN2 temperatures, the samples show brittle fracture. In several cases, minor kinks or irregularities appeared in the stress–strain curves due to brief recording artifacts from the load cell. These artifacts have been identified and adjusted in the reported curves to ensure that the data accurately reflect the material response. In some cryogenic tests, sharp drops or irregularities in the stress–strain and $(\Delta R/R)$ curves were observed due to specimen slippage during loading. These artifacts have been corrected in the revised plots, and future work will incorporate improved fixturing to prevent slippage under LN2 conditions. Piezoresistivity measurements revealed a consistent positive correlation between applied mechanical stress and the relative change in resistance $(\Delta R/R)$ at both temperatures. This behavior confirms the composite's piezo-resistive sensitivity. The bar plots summarize the mechanical properties (elastic modulus, ultimate tensile strength, and fracture strain) at both temperatures, as shown in Figure 4. At LN2 temperature, the elastic modulus increased by 120% and 71%, respectively, relative to room temperature, indicating

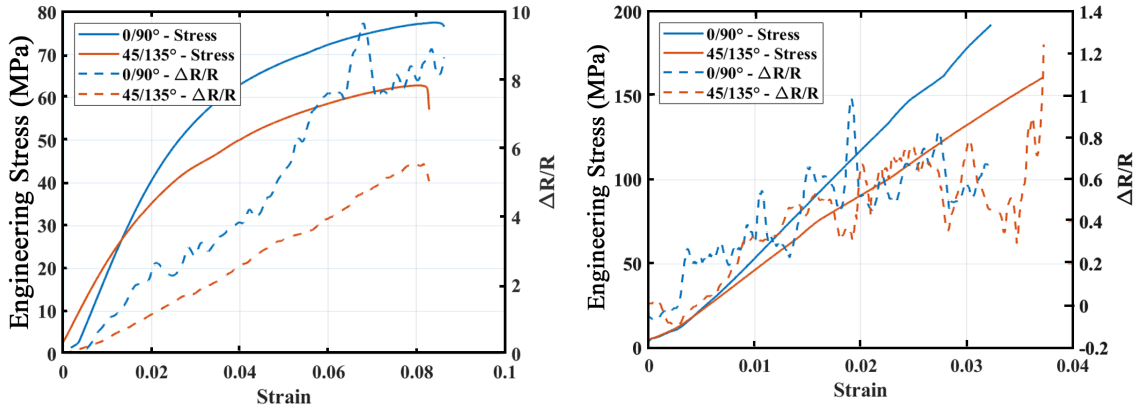

(a) Room Temperature (b) LN2 Temperature

Figure 3: Stress and normalized resistance change (ΔR/R) as a function of mechanical strain for different print orientations. The average baseline resistance is 2.12 kΩ at room temperature and 92.19kΩ at cryogenic temperature.

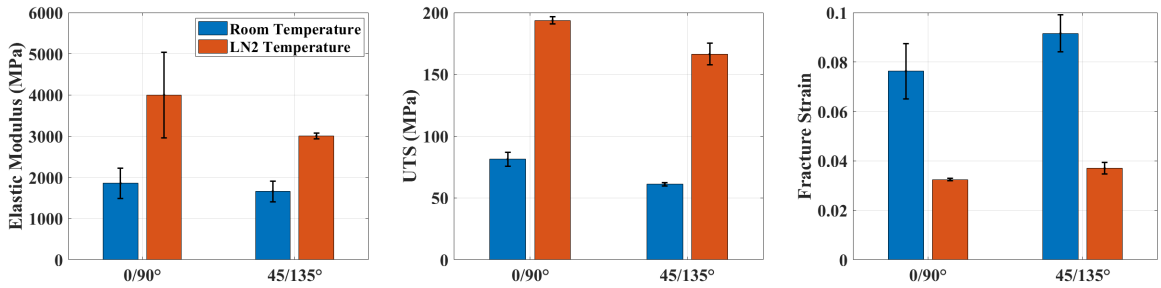

(a) Elastic Modulus (b) Ultimate Tensile Strength (c) Fracture Strain

Figure 4: Mechanical properties compared at room temperature and LN2 temperature. Each value represents the average of three tests for a given print parameter, with error bars indicating ±1 standard deviation from the mean.

enhanced stiffness under cryogenic conditions. Ultimate tensile strength (UTS) also showed substantial improvement, with increases of 150% and 160% for the respective orientations as shown in Figures 3 and 4.

3.2. Printing speed

The influence of print speed on the composite's mechanical and piezometric response was investigated by fabricating specimens at 50 mm/s, 100 mm/s, and 150 mm/s. The stress–strain response at room temperature exhibited typical elasto-plastic behavior with ductile failure and visible necking, whereas at LN2 temperature the specimens fractured in a brittle manner with little to no plastic deformation. The relative resistance change ($\Delta R/R$) at room temperature increased linearly up to the elastic limit, followed by an exponential rise at the onset of plasticity. In contrast, the $\Delta R/R$ curves at LN2 temperature showed greater fluctuation but generally maintained a linear increase with applied load. Across all conditions, resistivity measurements confirmed an increase in resistance under mechanical loading, with specimens printed at 100 mm/s showing the largest piezoresistive response, as presented in Figure 5. Tensile testing at LN2 temperature demonstrated significant increases in elastic modulus across all print speeds when compared to room temperature. Specifically, elastic modulus improvements were 316%, 124%, and 115% for 50 mm/s, 100 mm/s, and 150 mm/s, respectively. Ultimate tensile strength also increased markedly, with values rising by 124%, 100%, and 132%, respectively, at cryogenic temperature as shown in Figure 6.

3.3. Layer height

The effect of layer height on the mechanical and piezometric properties was assessed using specimens printed at 0.12 mm, 0.16 mm, and 0.2 mm layer thicknesses. Under LN2 conditions, the elastic modulus

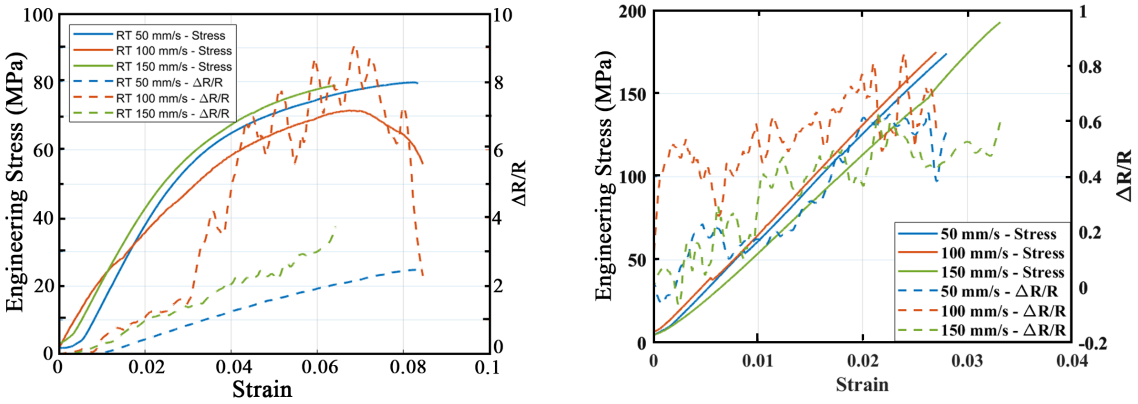

(a) Room Temperature (b) LN2 Temperature

Figure 5: Stress and normalized resistance change (ΔR/R) as a function of mechanical strain for different print speed. The average baseline resistance is 1.15 kΩ at room temperature and 9.3 kΩ at cryogenic temperature.

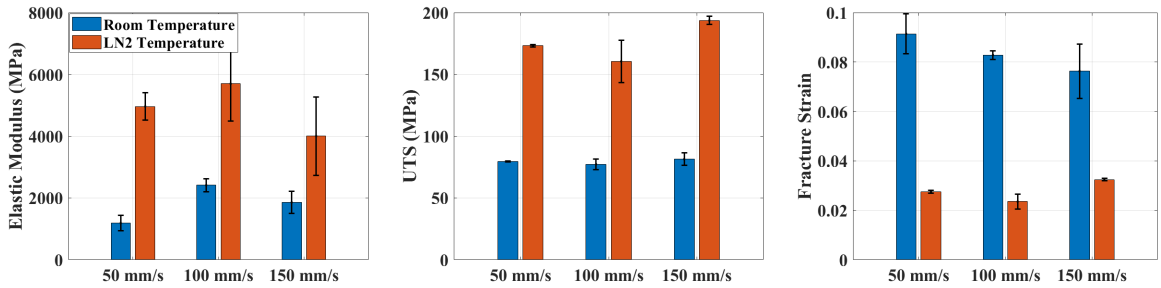

(a) Elastic Modulus (b) Ultimate Tensile Strength (c) Fracture Strain

Figure 6: Mechanical properties compared at room temperature and LN2 temperature. Each value represents the average of three tests for a given print parameter, with error bars indicating ±1 standard deviation from the mean.

increased by 180%, 140%, and 120%, respectively, relative to room temperature. Corresponding ultimate tensile strength values improved by 114%, 103%, and 138% as shown in Figures 7 and 8 The data reveals a clear trend at cryogenic temperature whereby specimens with greater layer height exhibited enhanced tensile strength. Resistivity measurements confirmed a strong positive correlation between mechanical load and $\Delta R/R$ across all layer heights and temperatures, consistent with prior observations. However, no statistically significant differences in piezoresistive response were detected between layer heights, indicating that layer thickness has minimal influence on the composite's piezo sensitivity under tensile loading.

4. Conclusion

This study demonstrated the distinct piezoresistive behavior of additively manufactured composite materials under both ambient and cryogenic temperature conditions, providing new insights into how printing parameters influence these properties. The results showed that increased layer height correlates with enhanced ultimate tensile strength (UTS), while a 0°/90° print orientation yields optimal mechanical performance. At room temperature, pronounced changes in piezoresistive response were observed at the onset of plasticity, regardless of printing conditions. At cryogenic temperatures, the piezoresistive response exhibited amplified piezo sensitivity compared to room temperature. These findings address a critical need in structural health monitoring for extreme-environment applications, particularly in aerospace, long-haul trucking, and energy storage systems, where traditional sensing approaches face significant limitations. Current monitoring solutions for cryogenic storage tanks and pipelines rely on external sensors that are prone to failure, require extensive wiring, and cannot provide distributed stress information throughout the structure. By contrast, the demonstrated piezoresistive properties enable the material itself to function as an integrated sensor, offering real-time stress detection capabilities without

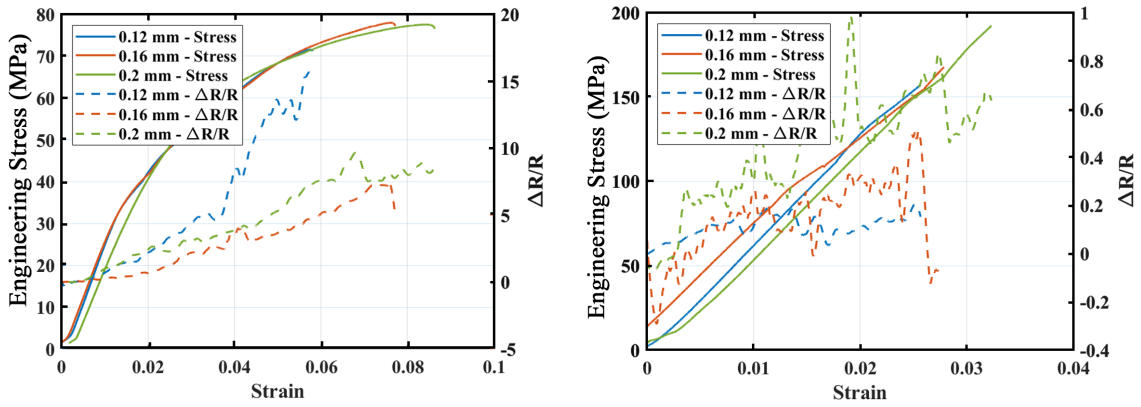

(a) Room Temperature (b) LN2 Temperature

Figure 7: Stress and normalized resistance change (ΔR/R) as a function of mechanical strain for different layer height. The average baseline resistance is 6.77 kΩ at room temperature and 47.8 kΩ at cryogenic temperature.

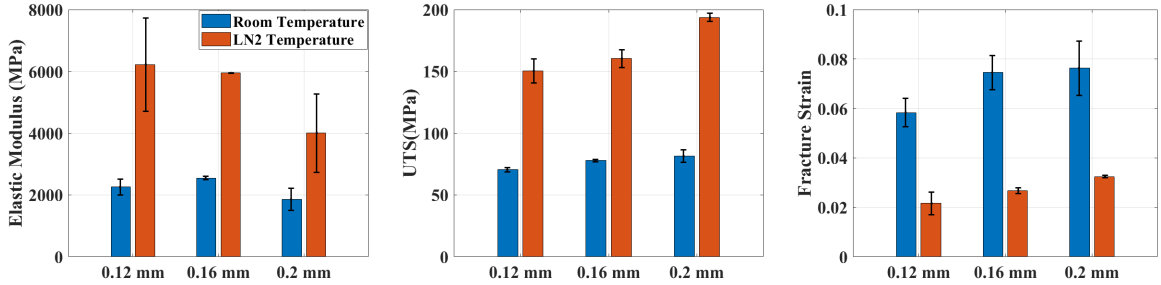

(a) Elastic Modulus (b) Ultimate Tensile Strength (c) Fracture Strain

Figure 8: Mechanical properties compared at room temperature and LN2 temperature. Each value represents the average of three tests for a given print parameter, with error bars indicating ±1 standard deviation from the mean.

additional hardware complexity. This self-sensing functionality is especially valuable in inaccessible or hazardous environments where sensor maintenance is challenging, and system reliability is vital. By eliminating the need for discrete sensing components while maintaining structural integrity, this composite material represents a paradigm shift toward intelligent infrastructure capable of autonomously monitoring its own health and predicting potential failure before it occurs.

Acknowledgments
We would like to thank Pallock Halder for his help with specimen preparation and testing and we would like to thank Robert Lentz for his assistance through the instrumentation process. Additionally, we would like to thank Professor Jacob Leachman, Zachary Beadle, and Reagan Dodge for their contributions to the project. The authors gratefully acknowledge the WSU start-up fund (PG00023149) to support this work.

References

[1] Ngo T, Kashani A, Imbalzano G, Nguyen K and Hui D, 2018, *Composites Part B: Engineering*, **143**, 172–196

[2] Attaran M, 2017, *Business Horizons*, **60(5)**, 677–688

[3] Zhou L, Miller J, Vezza J, Mayster M, Raffay M, Justice Q, Al Tamimi Z, Hansotte G, Sunkara L and Bernat J, 2024, *Sensors*, **24(9)**, 24092668

[4] Mojumder S, 2024, PhD thesis, Northwestern University

[5] Mojumder S, Suarez D, Abbott T and Liu W K, 2025, *Advanced Engineering Materials*, 2402592

[6] Ciampaglia A, Roccia S and Ciardiello R, 2024, *Composite Structures*, **353**, 118729

[7] Liu J, Lama G C, Recupido F, Santillo C, Gentile G, Buonocore G G, Verdolotti L, Zhang X and Lavorgna M, 2023, *Composites Science and Technology*, **236**, 109993

[8] AlMahri S, Schneider J, Schiffer A and Kumar S, 2022, *Polymer Testing*, **114**, 107687

[9] Gu D, Luo G, Zhou G, Zhou Y, Lou Y, Liang Y, Peng Y, Shen P, Pan B, Chen G and Wen B, 2024, *ACS Applied Electronic Materials*, **6**, 8203–8210

[10] Dios J R, Gonzalo B, Tubio C R, Cardoso J, Gonçalves S, Miranda D, Correia V, Viana J C, Costa P and Lanceros-Méndez S, 2020, *Macromolecular Materials and Engineering*, **305**, 2000379

[11] Tan J and Low H, 2020, *Additive Manufacturing*, **36**, 101551

[12] Getachew M, Shiferaw M and Ayele B, 2023, *Advances in Materials Science and Engineering*, **2023**, 8817006

[13] Wang F, Cooper N, Johnson D, Hopton B, Fromhold T M, Hague R, Murray A, McMullen R, Turyanska L and Hackermüller L, 2025, *arXiv preprint*, arXiv:2503.11570

[14] Hunt M, Salmon K, Haney J, Evans C, Gozen A and Leachman J, 2020, *IOP Conf. Ser.: Mater. Sci. Eng.*, **755**, 012118

[15] Poulaert B and Issi J P, 1983, *Polymer*, **24(7)**, 841–845

[16] ASTM International, 2014, ASTM D638-14, Standard Test Method for Tensile Properties of Plastics, *ASTM International*